

**The *Fasciola hepatica* thioredoxin: high resolution structure reveals two
oxidation states**

Kirsty Line¹, Michail N. Isupov¹, Esther Garcia-Rodriguez¹, Gabriela Maggioli²

Francisco Parra² & Jennifer A. Littlechild^{1*}

* Corresponding Author: Henry Wellcome Building for Biocatalysis, School of Biosciences, University of Exeter, Stocker Road, Exeter, EX4 4QD, UK, Tel: (+44) (0)1392 263468; Fax: (+44) (0)1392 263489; e-mail; J.A.Littlechild@exeter.ac.uk

1 Henry Wellcome Building for Biocatalysis, School of Biosciences, University of Exeter, Stocker Road, Exeter, EX4 4QD, UK.

2 Departamento de Bioquímica y Biología Molecular, Instituto Universitario de Biotecnología de Asturias, Universidad de Oviedo, Julian Clavería, 33006 Oviedo, Spain

Abbreviations

SOD – Superoxide dismutase

ES – Excretory/Secretory

Prx – Peroxiredoxin

Trx – Thioredoxin

TrxR – Thioredoxin reductase

Workers who have moved from institutions since work was performed:

Esther Garcia-Rodriguez; Gabriela Maggioli

Introduction

Fasciola hepatica is an important digenetic trematode common in ruminant livestock and increasingly causing infection in humans [1]. The infective life stage of the parasite, the metacercariae, excyst from a dormant state following ingestion by the host and penetrate the intestinal wall before migrating to the liver. They cause extensive damage to the liver prior to moving into the bile ducts. The flukes pass the bile duct walls and develop into their mature form that lives in the microenvironment of the bile ducts. The developing and migrating parasite is exposed to reactive oxygen species generated by the host effector cells such as macrophages, neutrophils, eosinophils and platelets [2, 3]. These cells generate free radicals via the oxidative burst and are thought to contribute to the killing of parasites by the host [3, 4, 5]. Previous studies have shown the presence of CuZn superoxide dismutase (SOD) activity in the excretory-secretion (ES) products of both immature and adult flukes [6], however, to date no catalase or glutathione peroxidase enzymes have been detected [7]. The action of SOD results in the production of hydrogen peroxide, which can readily diffuse widely and is potentially more damaging than superoxide. It is thought that the peroxiredoxin (Prx) and thioredoxin (Trx) enzyme system fulfils the role of peroxide metabolism in *Fasciola*, as proposed by McGonicle *et al* [8]. *Fasciola* Prx has been associated with protection against the by-products of aerobic metabolism [9] and the natural electron donor of this enzyme is Trx. Trx is a ubiquitous small protein (typically around 12 kDa) which contains a redox active disulfide. Reducing equivalents ultimately come from NADPH, via the flavin dependent enzyme thioredoxin reductase (TrxR). Reduced Trx is known to interact with and reduce a number of proteins and metabolites.

All members of this protein family have a similar structure, the Trx fold, which has a central five stranded β sheet surrounded by four α helices. Classical Trxs have the active site motif containing the conserved cysteine residues (Trp-Cys-Gly-Pro-Cys) which is located between β strand 2 and α helix 2 [10]. Trx is essential to a number of cellular functions and is an important protein in protection against oxidative stress. It supplies reducing equivalents to a number of enzymes such as Prx, ribonucleotide reductase and also reduces cysteine residues in other proteins [11], including transcription factors which result in their increased binding to DNA [10].

The human Trx1 oxidising activity has been shown to be regulated by a number of factors in different cells. In endothelial cells the S-nitrosylation of residue C69 has been shown to be essential for the apoptotic function and redox regulation of Trx1 [12]. Additionally, during oxidative stress residue C73 has been shown to be glutathionylated, reducing the Trx activity [13]. A further disulfide motif between residues C62 and C69 has also been identified in human Trx1 which can impair Trx activity during redox signalling and oxidative stress, allowing for more time for the sensing and transmission of the oxidative signal [14].

F. hepatica Trx was identified as a tegumental antigen being present on both juvenile and adult worm stages of *Fasciola* [15]. The 12kDa protein was subsequently cloned, over expressed and functionally characterised [16]. Here we describe the x-ray crystal structure of this recombinant thioredoxin protein solved to 1.45 Å.

Materials and Methods

Protein Sample and Crystallisation

A *Bam*HI restriction fragment from plasmid pGEX-TRX [16], containing the *F. hepatica* Trx coding sequence, was cloned into plasmid pQE30 previously digested with *Bam*HI, resulting in pQE-*Fh*Trx expression vector. The correct orientation of the cDNA insert was investigated by restriction analysis and nucleotide sequencing. Recombinant Trx was expressed and purified from *E. coli* BL21 cultures transformed with pQE-*Fh*Trx vector and induced for 3 hours with 0.2 mM isopropyl- β -D-thiogalactoside at 37°C. Cells were harvested by centrifugation, suspended in cold phosphate saline buffer (PBS) and then lysed by sonication. The extract was clarified by centrifugation and loaded onto a Ni-Sepharose column equilibrated in 0.1 M PBS buffer pH 7.0. The column was serially washed with PBS containing increasing concentrations of imidazole and the recombinant Trx was finally eluted with 400 mM imidazole. The pooled fractions containing recombinant Trx were dialyzed against 50 mM potassium phosphate buffer, 140 mM sodium chloride, pH 7.4. Protein was precipitated by 70% (saturation) ammonium sulfate for the purpose of storage and shipment. The precipitated protein was resuspended in 50 mM potassium phosphate buffer, 140 mM sodium chloride, pH 7.4 and dialysed against the same buffer to ensure removal of all of the ammonium sulfate. The recombinant protein was concentrated to ~ 9 mg/ml in 50 mM potassium phosphate buffer, 140 mM sodium chloride, pH 7.4 using Amicon Ultra-4 5000 molecular weight cut off (MWCO) centrifugal filtration devices (Millipore). Crystals were successfully grown by vapour diffusion using the Molecular Dimensions Limited Structure Screen 1, condition number 32 (0.1M Tris-HCl pH 8.5 and 2 M ammonium sulfate). Crystallisation trays were incubated at 19 °C and crystals grew within 5 days. Crystals were harvested

into a cryo-liquor containing 0.1M Tris-HCl pH 8.5, 55% (saturation) ammonium sulfate and 30% (v/v) glycerol, and flash frozen in liquid nitrogen.

X-ray data collection, processing, structure solution and refinement

The crystals diffracted to 1.3Å resolution and were found to belong to the space group $P2_1$ with the unit cell parameters $a = 32.67 \text{ \AA}$, $b = 34.59 \text{ \AA}$, $c = 40.38 \text{ \AA}$, $\alpha = \gamma = 90^\circ$ and $\beta = 106.3^\circ$. Data were collected at the BW6 beamline of HASYLAB (DESY, Hamburg) under cryo-cooled conditions (100 ° K). Data to 1.45 Å resolution were processed, and scaled using the programs DENZO and SCALEPACK [17]. The *Fasciola* Trx structure was solved by molecular replacement using the program BABEL [18,19]. The solution chosen used the search model 2fa4, the 2.38 Å thioredoxin structure from *Saccharomyces cerevisiae* [20]. Refinement was carried out using the program REFMAC 5.2 [21]. The model building was performed using COOT [22]. Structure analysis was carried out using COOT [22] and PyMol [23]. The root mean squared standard deviations (RMSDs) between different structures were calculated using the program O [24]. The structure has been deposited at the wwwPDB and assigned the code 2vim.

Results and Discussion

Structural analysis and quality of the model

The crystal structure of the recombinant *Fasciola* Trx has been determined at 1.45 Å resolution. The data and refinement statistics are shown in table 1. The asymmetric unit contains a monomer. The final R value is 0.19 and the R_{free} value 0.24 with good stereochemistry. 91.5% of the residues fall within the allowed regions of the Ramachandran plot as defined by PROCHECK [25]. The remaining 8.5% of residues fall into the additionally allowed regions. All amino acid residues could be located in the electron density and the side chains of residues Cys31, Cys34, Glu50, Glu62, Ser69, Met73, Asp81, and Lys 95 were found to occupy two positions. The side chain of Ser89 was found to occupy three positions. 106 water molecules were modelled.

Overall structure

The overall structure of *Fasciola* Trx is shown in figure 1, and the secondary structure elements are indicated on the sequence alignment shown in figure 2. The general fold consists of a five stranded β -sheet surrounded by four α -helices (β - α - β - α - β - α - β - α). The molecular architecture of this Trx is similar to that seen in the structures of previously studied Trx proteins. There is a *cis* peptide between Met73 and Pro74. Many Trx fold proteins contain a conserved *cis* proline at this position which is thought to prevent the binding of metals to the active site thiolates [26]. As the *F. hepatica* Trx sequence only has the two catalytic cysteine residues (C31 and C34) it is unlikely that this Trx enzyme is involved in the regulatory processes seen for the human Trx counterpart. These additional cysteine residues are conserved in the Trx sequences found in the bovine and ovine host animals indicating that the Trx proteins

from these organisms are involved in similar regulation processes to those seen in the human system.

Active site

The active site of Trx enzymes contain a redox active cysteine pair (Cys31 and Cys34) which can be in the oxidised disulfide state or in the reduced dithiol state. The electron density of the *Fasciola* Trx structure shows the cysteine residues in both the disulfide and dithiol states (figure 3a and 3b). In the dithiol form the S^γ atoms are at a distance of 3.44 Å and in the disulfide form a distance of 2.23 Å. There appears to be only a small conformational change of the cysteine side chain positions in order to change between the two oxidation states. Cys31 Cβ has a movement of 0.39 Å and the S^γ atom rotates by 5.26° about Cβ, resulting in a movement of a distance of 0.8 Å between positions. Residue Cys34 has a smaller movement, the Cβ has a movement of 0.12 Å and the S^γ atom rotates around Cβ by 1.65° resulting in a movement of 0.5 Å between positions. Cys31 is exposed at the protein surface whereas Cys34 is in a more buried position. Cys34 S^γ atom in the dithiol state is at a distance of 3.39 Å from water molecule 71. Cys31 S^γ atom in the dithiol state is hydrogen bonded to water molecule 66 at a distance of 2.72 Å.

Comparison with other Trx structures

The *F. hepatica* Trx structure was found to be similar to other Trx structures and the RMSDs to the *F. hepatica* Trx are shown in table 2. The sequence identities of these proteins to *F. hepatica* Trx as calculated by BLAST [27] are also shown in table 2 and an alignment is shown in figure 2. Also shown in the alignment are the Trx sequences from two host animals *Bos taurus* and *Ovis aries*.

The positions of the active site Cys residues are similar to those seen for other structures of Trx showing both disulfide and dithiol oxidation states. The active site contains a conserved Trp residue which is present in the conserved Trx motif sequence (WCGPC). This residue is on the surface of the protein, and in most Trx structures is found to form a flat surface close to the active site [32]. In the *T. brucei* structure this residue is flipped out and interacts with a neighbouring protein molecule in the crystals [32], demonstrating that the Trp residue can adopt different conformations; possibly when the Trx is interacting with one of its redox partners [32]. In the *F. hepatica* Trx structure Trp30 is positioned so as to form a flat surface. In all of the structures listed in table 2 with the exception of the *T. brucei* structure, this residue is positioned with the side chain flat to the protein surface.

Trx proteins generally contain a conserved Asp residue in the active site behind the more buried Cys residue. Most of the Trx structures that show this conserved Asp residue also have a water molecule bonded to one of the Asp carboxylate oxygen atoms. In *F. hepatica* Trx both carboxylate oxygen atoms of Asp25 are bound to water molecules; water 71 is 2.6 Å from atom OD1 and water 13 is 2.6 Å from atom OD2. The most conserved water of these two in the other structures shown in table 2 is water 13, with an equivalent water molecule being found in the Trx structures PDB 1xwa, 1ert, 1xwb, 1xw9, 1xwc and 2fa4, that are all at a distance between 0.29 Å and 1.1 Å from the position of water 13. The *T. brucei* protein (PDB 1r26) does not have the conserved Asp residue, having a Tyr residue instead and has a water molecule positioned between the positions of water 13 and water 71 of the *F. hepatica* Trx structure. In the *F. hepatica* Trx structure Cys31 S^γ atom in the dithiol state is

hydrogen bonded to water molecule 66, which does not seem to have equivalent water molecules in any of the structures shown in table 2.

In the *Drosophila melanogaster* Trx structures, residue Phe28 was seen to move over the active site Cys35 in two of the oxidised state structures [31]. The authors propose that in this position the Phe residue may be blocking movement of Cys35 when the side chain of C32 approaches during oxidation [31]. In most structures the equivalent Phe residue side chain is found to be positioned away from the active Cys pair, as is the case in the *F. hepatica* Trx structure (Phe27). In The human Trx1 protein the equivalent residue at this position is a Ser (Ser28) and in the *T. brucei* Trx the equivalent residue is a Thr (Thr26).

Summary

This study has provided detailed structural analysis of the *F. hepatica* Trx which has demonstrated the subtle conformational changes associated with its oxidation from the free thiol to the disulfide form. This information provides a useful comparison with the human Trx protein, and by sequence identity to the Bovine and Ovine Trx's, the hosts of the parasite. Further studies are in progress to investigate the detailed interaction of the *F. hepatica* Trx and the peroxiredoxin to understand details of the oxidative stress response induced during the parasite infective cycle.

Despite having 66% sequence identity the RMSD of the *F. hepatica* and the human Trxs is very similar at 0.57 (reduced) and 0.6 (oxidised). The *F. hepatica* Trx crystal structure shows a mixture of both oxidised and reduced cysteines within the same

crystal, demonstrating the small conformation changes between these two states. This is the only Trx structure that shows both the oxidation states in the same structure. Interestingly the *F. hepatica* Trx structure shows highest identity to the human and therefore higher eukaryote Trx structures than to those of lower eukaryote organisms. This study has allowed a detailed structural comparison of the Trx protein from *F. hepatica* with Trxs from two other parasites. It also provides a comparison with the host Trx proteins from human, and by high sequence identity, to bovine and ovine species. The study has shown that the *F. hepatica* Trx crystal structure is most similar to the Trx from the human host. The *F. hepatica* Trx resembles other lower eukaryotic Trxs in that it does not have additional cysteine residues present in the host Trxs that are proposed to be involved in regulatory processes associated with higher eukaryotes. Further studies providing information on protein/protein complexes of Trx with other proteins from both the parasite and host will provide additional information regarding the role of the *F. hepatica* Trx in oxidative stress and parasitic adaptation.

Acknowledgments

We would like to thank the EU FP6 for funding KL. We acknowledge support under the European Community Access to Research Infrastructure Action of the Improving Human Potential Programme to EMBL Hamburg Outstation, contract number HPRI-CT-1999-0017. GM was a fellow from Agencia Española de Cooperación Internacional (MAEC-AECI).

References

- [1] McManus D, Dalton JP. Vaccines against the zoonotic trematodes *Schistosoma japonicum*, *Fasciola hepatica* and *Fasciola gigantica*. *Parasitology* 2006;133:S43-S61.
- [2] Badwey JA, Karnovsky ML. Active oxygen species and the functions of phagocytic leukocytes. *Annu Rev Biochem* 1980;49:695-726.
- [3] Maizels RA, Bundy DAP, Sle Kirk ME, Smith DF, Anderson RM. Immunological modulation and evasion by helminth parasites in human populations. *Nature* 1993;365:797-805.
- [4] Murray HW. Susceptibility of *Leishmania* to oxygen intermediates and killing by normal macrophages. *J Exp Med* 1981;153:1302-1315.
- [5] Nathan C, Nogueira N, Juangbhanich C, Ellis J, Cohn ZA. Activation of macrophages *in vivo* and *in vitro*. Correlation between hydrogen peroxide release and killing of *Trypanosoma cruzi*. *J Exp Med* 1979;149:1056-1068.
- [6] Piacenza L, Radi R, Goni F, Carmona C. CuZn superoxide dismutase activities from *Fasciola hepatica*. *Parasitology* 1998;117:555-562.
- [7] Maggioli G, Piacenza L, Carambula B, Carmona C. Purification, characterisation, and immunolocalisation of a thioredoxin reductase from adult *Fasciola hepatica*. *J. Parasitol* 2004;90:205-211.
- [8] McGonicle S, Curley GP, Dalton JP. Cloning of peroxiredoxin, a novel antioxidant enzyme, from the helminth parasite *Fasciola hepatica*. *Parasitology* 1997;115:101-104.
- [9] Salazar-Calderón M, Martín-Alonso, JM, Ruiz de Eguino AD, Casais R, Marín MS, Parra F. *Fasciola hepatica*: heterologous expression and functional characterisation of a thioredoxin peroxidase. *Exp Parasitol* 2000;95:63-70.

- [10] Arnér ESJ, Holmgren A. Physiological functions of thioredoxin and thioredoxin reductase. *Eur J Biochem* 2000;267:6102-6109.
- [11] Rahlfs S, Schirmer RH, Becker K. The thioredoxin system of *Plasmodium falciparum* and other parasites. *Cell Mol Life Sci* 2002;59:1024-1041.
- [12] Haendeler J, Hoffmann J, Tischler V, Berk CB, Zeiher AM, Dimmeler S. Regulation of telomerase activity and anti-apoptotic function by protein-protein interaction and phosphorylation. *Nature Cell Biol* 2002;4:743-749.
- [13] Casangrande S, Bonetto V, Fratelli M, Gianzza E, Eberini I, Massignan T, Salmons M, Chang G, Holmgren A, Ghessi P. Glutathionylation of human thioredoxin: a possible crosstalk between glutathione and thioredoxin systems. *Proc Natl Acad Sci USA* 2002;99:9745-9749.
- [14] Watson WH, Pohl J, Montfort WR, Stuchlik O, Reed MS, Powis G, Jones DP. Redox potential of human thioredoxin 1 and identification of a second dithiol/disulfide motif. *J Biol Chem*, 2003;278:33408-33415.
- [15] Shoda LK, Rice-Ficht AC, Zhu D, McKown RD, Brown WC. Bovine T-cell responses to recombinant thioredoxin of *Fasciola hepatica*. *Vet Parasitol* 1999;82:35-47.
- [16] Salazar- Calderón M, Martín-Alonso JM, Ruiz de Eguino AD, Parra F. Heterologous expression and functional characterisation of thioredoxin from *Fasciola hepatica*. *Parasitol Res* 2001;87:390-395.
- [17] Otwinowski Z, Minor W. Processing of X-ray diffraction data collected in oscillation mode. *Methods Enzymol* 1997;276:307-326.
- [18] Long F, Vagin A, Young P, Murshudov GN. BALBES: a molecular replacement pipeline. *Acta Crystallog* 2007;D63:to be published.

- [19] Collaborative Computational Project Number 4. The CCP4 suite programs for protein crystallography. *Acta Crystallogr* 1994;D50:760-763.
- [20] Bao R, Chen Y, Tang YJ, Janin J, Zhou CZ. Crystal structure of the yeast cytoplasmic thioredoxin Trx2. *Proteins* 2007;66:246-249.
- [21] Murshudov GN, Vagin AA, Dodson EJ. Refinement of macromolecular structures by the maximum-likelihood method. *Acta Crystallog* 1997;D53,:240–255.
- [22] Emsley P, Cowtan K. Coot: model-building tools for molecular graphics. *Acta Crystallogr* 2004;D60:2126-32.
- [23] Delano WL. DeLano Scientific, San Carlos, CA, USA, 2002; <http://www.pymol.org>.
- [24] Jones TA, Zou JY, Cowtan SW, Kjeldgaard M. Improved methods for building protein models in electron density maps and the location of errors in these models. *Acta Crystallogr* 1991;A24:945-949.
- [25] Laskowski RA, MacArthur MW, Moss DS, Thornton, J.M. PROCHECK: a program to check the stereochemical quality of protein structures. *J Appl Crystallog* 1993;26:283-291.
- [26] Gouet P, Courcelle E, Stuart D.I. Metz F. ESPript: multiple sequence alignments in PostScript. *Bioinformatics* 1999;15: 305-8.
- [27] Su D, Berndt C, Fomenko DE, Holmgren A, Gladyshev VN. A conserved *cis*-proline precludes metal binding by the active site thiolates in members of the thioredoxin family of proteins. *Biochemistry* 2007;46:6903-6910.
- [28] Tatusova TA, Madden TA. Blast 2 sequences - a new tool for comparing protein and nucleotide sequences. *FEMS Microbiol Lett* 1999;174:247-250.
- [29] Thompson JD, Higgins DG, Gibson TJ. ClustalW: Improving the sensitivity of progressive multiple sequence alignment through sequence weighting, position-

specific gap penalties and weight matrix choice. *Nucleic Acids Res* 1994;22:4673-4680.

[30] Weicshel A, Gasdaska JR, Powis G, Montford WR. Crystal structures of reduced, oxidised and mutated human thioredoxins: evidence for regulatory homodimer. *Structure* 1996;4:735-751.

[31] Wahl MC, Irmeler A, Hecker B, Schirmer RH, Becker K. Comparative structural analysis of oxidised and reduced thioredoxin from *Drosophila melanogaster*. *J Mol Biol* 2005;345:1119-1130.

[32] Friemann R, Schmidt H, Ramaswamy S, Forstner M, Krauth-Siegel RL, Eklund H. Structure of thioredoxin from *Trypanosoma brucei brucei*. *FEBS Lett* 2003;554:301-305.

[33] Robien MA, Hol WGJ. Protozoa, Structural Genomics of Pathogenic Initial Structural Analysis of *Plasmodium falciparum* thioredoxin. PDB deposition April 2004. www.pdb.org

Figure legends

Figure 1 Cartoon representation of *F. hepatica* Trx with secondary structure elements labelled in addition to the N and C termini. The figure was generated with PyMol [23].

Figure 2 Clustal alignment of Trx sequences from *F. hepatica*, *B. taurus*, *O. aries*, *H. sapiens*, *S. cerevisiae*, *D. melanogaster*, *T. brucei* and *P. falciparum*. Identical residues are in shaded blocks, similar residues are in outlined boxes. Secondary structure elements of the *F. hepatica* Trx are shown above the alignment. The asterisks above residues indicate sidechains which have a second position in the structure and the 1 below the cysteine residues indicates the presence of a disulfide bond. The figure was generated in ESPript [26].

Figure 3 (a) Stereo view of a cartoon representation showing the active site cysteine residues (labelled) in the disulfide oxidation state. The secondary structure elements are shown in green, the cysteine residues are shown as sticks with the sulfur atoms coloured yellow. The figure was generated with PyMol [23]. (b) Stereo view of a cartoon representation showing the active site cysteine residues (labelled) in the sulfoxide oxidation state. The secondary structure elements are shown in green, the cysteine residues are shown as sticks with the sulfur atoms are coloured yellow. The figure was generated with PyMol [23].

Table Legends

Table 1 Summary of data collection and refinement statistics.

Table 2 Structural alignment RMSD and sequence identities for different Trx structures versus the *F. hepatica* Trx

Table 1

Summary of data collection and refinement statistics

Space Group	P1 2 ₁ 1
Unit cell parameters (Å)	a = 32.67, b = 34.59, c = 40.38, $\alpha = \gamma = 90^\circ$ and $\beta = 106.3^\circ$
Resolution Range (Å)	38.69 – 1.38
Completeness (%)	89.65
R_{sym} (last shell)	0.072 (0.488)
$\langle I \rangle / \langle \sigma I \rangle$ (last shell)	10.75 (0.87)
Redundancy	2.4
Unique reflections	16069
<i>B</i> -factor of data from Wilson plot (Å ²)	25.94
Final R_{cryst} (%)	19.2
R_{free} (2.0% total data: %)	24.8
No. of protein residues	104
Average <i>B</i> -factor (protein: Å ²)	24.22
No. water molecules	103
Average <i>B</i> -factor (water: Å ²)	40.37
Rms deviations from ideality ^a	
Bond lengths (Å)	0.017 (0.022)
Bond angles (°)	1.679 (1.968)
<i>B</i> -factors correlation (Å ²) ^a	
Main-chain bond	2.627 (4.0)
Main-chain angle	3.696 (6.0)
Side-chain bond	4.860 (8.0)
Side-chain angle	7.357 (10.0)

$R_{\text{sym}} = \sum |I - \langle I \rangle| / \sum I$, $R_{\text{cryst}} = \sum ||F_o| - |F_c|| / \sum |F_o|$ where *I* is the intensity of the reflection.

^a Target values are given within parentheses.

Table 2

PDB	Organism	RMSD	No C α atoms	Sequence identity (%)	Reference
2fa4	<i>S. cerevisiae</i>	0.79	103	48	18
1ert (reduced)	<i>H. sapiens</i>	0.57	104	66	35
1eru (oxidised)	<i>H. sapiens</i>	0.60	104	66	35
1xwa	<i>D. melanogaster</i>	0.88	104	45	36
1r26	<i>T. brucei brucei</i>	1.12	101	43	37
1syr	<i>P. falciparum</i>	1.02	103	39	38

Figure 1

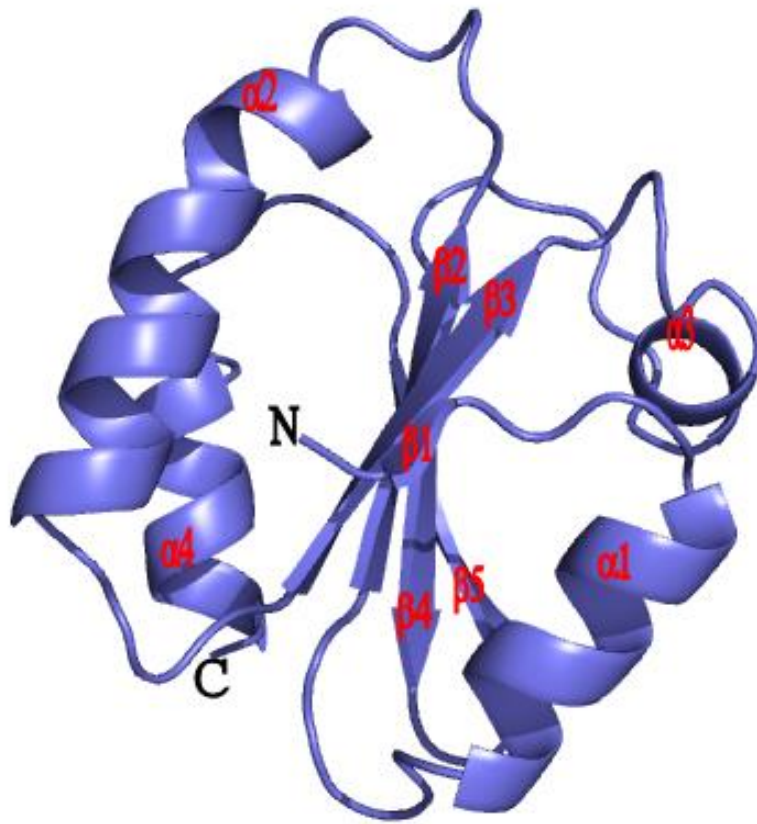


Figure 2

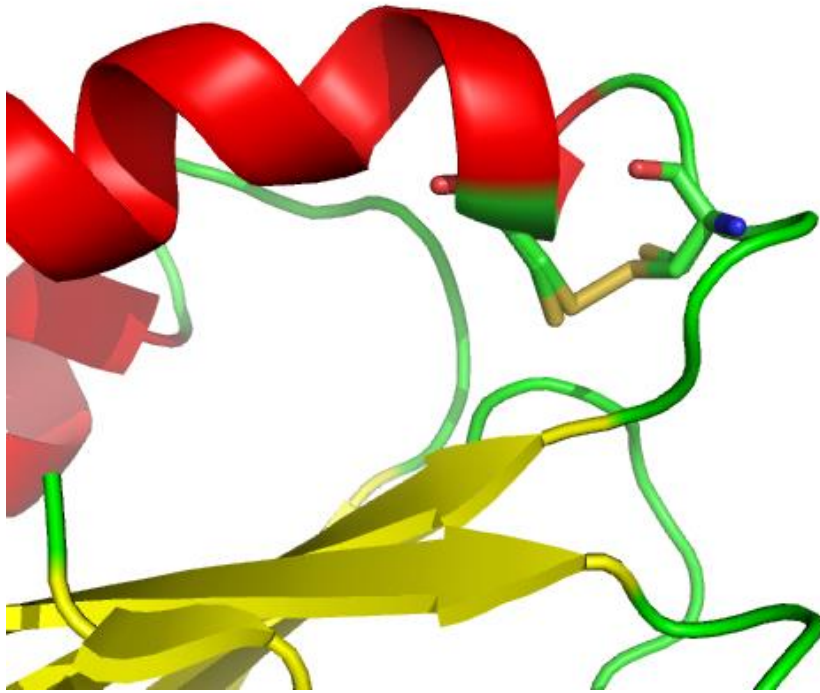


Figure 3

